Available online at www.sciencedirect.com
SCIENCE DIRECT®
Optics & Laser Technology 35 (2003) 505–515
Optics & Laser Technology
www.elsevier.com/locate/optlastec

# A new image processing method for evaluating the pupillary responses in a HMD-type eye-tracking device

Chern-Sheng Lin[a,*], Li-Wen Lue[a], Mau-Shiun Yeh[b], Thong-Shing Hwang[a], Su-Hsin Lee[c]

[a] *Department of Automatic Control Engineering, Feng Chia University, Taichung, Taiwan, ROC*
[b] *Chung-Shan Institute of Science & Technology, Lung-Tan, Tao-Yuan, Taiwan, ROC*
[c] *Department of Architecture, Feng Chia University, Taichung, Taiwan, ROC*

Received 14 October 2002; received in revised form 6 March 2003; accepted 24 March 2003

**Abstract**

In this paper, a new image processing method for evaluating the pupillary responses is described. This system is based on an eye-tracking system, using eye tracking and pattern recognition techniques with appropriate hardware and software. This pupillary response evaluation system includes a head-mounted display and a pinhole CCD camera. When the subject uses the head-mounted display to browse the screen of a computer, the CCD camera catches images of the subject's eye and transmits it to the computer. The program in the computer calculates the location and size of the pupil in the images. The pupil area calculation weighting function, visual fatigue detection, concentration detection, and eye/HMD slide compensation are included in the system. This allows the system to detect the pupil under different conditions. This system will know if anyone is using the system, then it evaluates the operating conditions of the subject, if the adjustment is correct, and guides the operator in using the system. The experimental results verified that this image system provides an economical and effective method for evaluating pupillary responses.


*Keywords:* Pupillary responses; Eye-tracking system; Head-mounted display

## 1. Introduction

An eye-tracking interface to determine the position of a user's pupil and map this position into a point on a display screen is proposed [1–3]. This new human–machine interface may not only solve many problems of people's lives but also play an important role in the control field. With eyeball tracking, any change in the eyes can become a new command. The applications for this eye-tracking system include a computer interface design evaluation, computer interface control, and aid control for the disabled. The data can also provide quantified information for ophthalmology and psychology uses.

In military applications, a combination of heads-up display (HMD) and eye-tracking device for guiding weapons systems frees the pilot's hands for fighting tasks. Usually, the device includes a detection device to detect bio-electromagnetic signals or image sequences generated by eye movements. Some eye-tracking techniques, which use contact lenses with induction coils, are so obtrusive that they cannot be used for extensive periods and are thus useless outside the laboratory. The optical one-point-type eye-tracking device can measure the eye movements of subjects who are seated in front of its infrared (IR) emitter, which uses a non-contact method to obtain the Perkinje image. As shown in Fig. 1, rays 1 and 4 of a Perkinje image are useful for monitoring the eye. The pupil and cornea appear as a bright spot and a glint to an optical IR sensor. The relationship between the pupil's center and the IR glint provides an eye-tracking system with gaze direction.

The eye-tracking system that we adopted has another setup. A CCD captures the eye images and sends them to an image capture card (Fig. 2). These images are then transmitted into a PC for processing. A PC to TV encoder box can simultaneously display a computer graphics video graphic array (VGA) signal both on a PC monitor and an HMD. A switch is used to select the video cassette recorder (VCR) image or the "VGA" output of a compatible PC for the user. Monitoring the pupillary response using this setup has the advantage of being inexpensive, non-intrusive, automated, and more serviceable. A pupil-meter is a device intended

* Corresponding author. Tel.: +886-4-4517250; fax: +886-4-4519951.
*E-mail address:* cslin@auto.fcu.edu.tw (C.-S. Lin).

0030-3992/03/$ - see front matter © 2003 Elsevier Science Ltd. All rights reserved.
doi:10.1016/S0030-3992(03)00063-X

to measure the pupil diameter using reflected light, but this system is expensive.

Generally, techniques for evaluating pupillary response can be classified into: (1) measuring the eye blink rate and (2) measuring the pupil dilation to determine its relationship with the information processed during vision attention, i.e. watching a program or engaging in a task. For example, in the eye-tracking experiments by Lin et al. [4], a new search method, superior to the existing methods, was used. The eye opening and closing actions activate additional commands, used for controlling robots. In order to save much search time in the face's image, this system uses many checkers to search effectively in the binary shadows. When coming across other features, it can quickly skip over them without detailed template comparison. The method is called diagonal-box checker search. This system allows the handicapped an opportunity to perform some simple tasks without the help of others. Wagner and Galiana [5] adopted the template matching with correlation calculation to find the locations of the eyes. Spindler and Chaumette [6] used an off-line calibration and gazed coordinates filtering for a visual serving task. Grattan and Palmer [7] and Grattan et al. [8] developed a microcomputer-based system for the disabled that relies upon differential reflection from the eyeball. The input blink is used to activate the data presentation as a binary tree or matrix scan. Over the past 30 years, consumer psychologists and marketing researchers have used pupillometrics to design, advertise and test new products [9]. The degree of interest can be measured by recording the pupil size. Stewart established a physiological measurement of advertising effect database to show that pupillary response is related to the information-processing demands of a task [10].

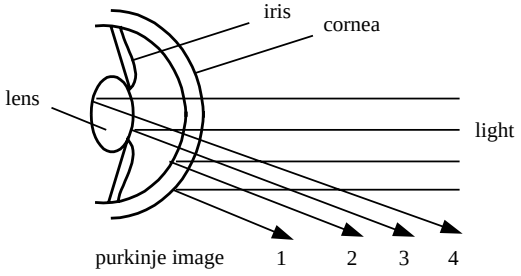


Fig. 1. Purkinje images.

In incident visible light, the pupil of the eye is the black center of the iris. The pupil allows light to enter the eye by neurological input to the iris muscles which control the pupil diameter. In a bright environment the pupil may be constricted into an opening less than 2 mm in diameter. In a dim environment the pupil may widen to over 8 mm. Such a change represents about a 17-fold increase in the pupil area. The pupil changes size in response to not only the ambient but also visual fatigue, excitement, etc. That means that signals from the eye during focusing also affect the size of the pupil. When someone is doing close task, the pupil shrinks to sharpen the image. On the contrary, the pupil becomes larger when one is watching a distant object. Extensive use of pupillary constriction can be made for researching the attention and cognitive efforts of human beings. A pupilometer is a device that is strapped to the head of a subject with an optical sensor aimed at his eye [11]. When the head movements are much slower than the iris movements, Xie et al. [12] presented a method for compensating head movements by using cascaded tracking of the white region and the dark region in the eye's image. Martin and Schovance [13] create the musculotendon dynamics and the plant model of the eye by using many biomedical informations including position and velocity of eye, velocity of agonist muscle contraction

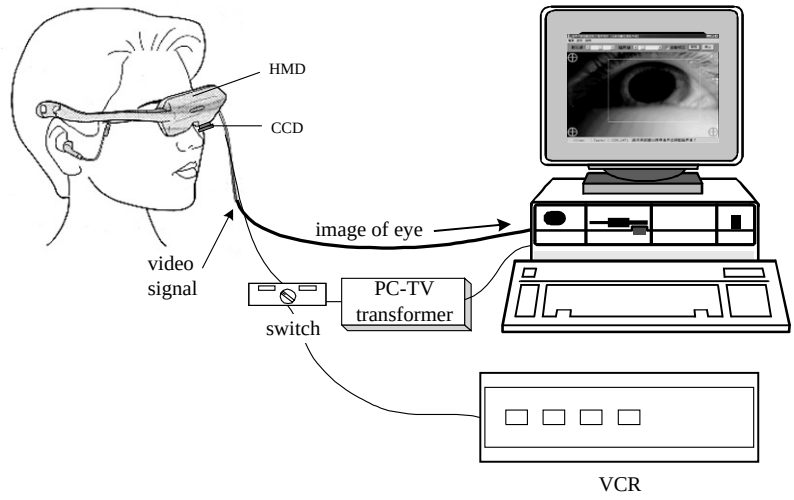


Fig. 2. The set up for measuring the pupillary responses.

and antagonist activation. Allison et al. [14], used an integrated head and eye tracking system to investigate the compensatory vestibulo-ocular responses. The measurement of three-dimension viewing behavior requires relatively large computational effort. Talmi and Liu used highlight detection and displacement vector transformation in the determination of the 3-D eye position [15]. In 3-D visualization of multimedia systems, eye blinking can be detected by calculating the values of the squared frame differences (SFD) of the blocks of the facial image [16]. We can find that the human visual tracking and evaluating system is a field of significant interest and importance.

Here, a new image-processing method is proposed for calculating the location and size of the pupil using inexpensive optical hardware. This pupillary response evaluation system also provides compensation approaches to correct potential experimental errors. As a result, the proposed method can improve the accuracy of the pupil area measurement and decrease the computational task. These will be the objectives of this paper.

## 2. Digital image processing method

### 2.1. Optical detection system

The PC can analyze and calculate the pupil opening and direction of a subject. This measuring system provides a pupil-analyzing program to determine the diameter of a pupil in real time. After the program is initiated, an image is captured for judgement to determine the operating conditions. The method for judging if the HMD and the CCD camera are set to the correct position is to create four lattice images (which are adjustable and typically $80 \times 80$ pixels ) per unit time, and then process each lattice image individually (Fig. 3). In the experiments, we find the image contrast is the best in red color channel if the user's eye is black. We obtain normalized red colour values $g_r$ from the gray-level $R$, $G$ and $B$ colors of an image.

$$g_r = \frac{R}{R+G+B}.$$

Let

$$S_{i,j} = \frac{\sum g_r}{n},$$

$$V_j = |S_{i,j} - S_{i-1,j}| \times 0.25 \quad j = 1 \sim 4,$$

$$V_t = V_1 + V_2 + V_3 + V_4,$$

where $g_r$ is the gray level of the pixel red color, $S_{i,j}$ is the average gray level of the red color of the $j$th lattice image in $i$th image sequence, $n$ is the pixel number of a lattice image, and $V_j$ is the variation in the average gray level of the red color of the $j$th lattice image

The variation in the average gray level of the lattice image $V_t$ red color is larger than a specified data. When $V_t$ is small, we can infer that there may be no subject wearing the HMD device in the pre-operation condition. If the average gray level of the red color of the lattice image $S_{i,j}$ is within a specified range, the program continues. If all of the average gray levels of the lattice image are within range, the program continues. If not, a digital movie file in AVI format will display how to place the hardware. While the HMD is in use, the value $V_t$ is calculated per minute. The system then insures that there is no variation in the four lattice images to insure there is no slide between the eye and the CCD.

### 2.2. The pupil area calculation weighting function

In Fig. 4, we can see that the shadow appears at the lower-left when the user gazes at the right icon (the pupil move to the left in the image). The shadow appears in the right when the user gazes at the left icon, the top when the user gazes at the top icon, and at the bottom when the user gazes at the bottom icon. The shadow appears as dark as the pupil and will calculate the error from the center of the pupil. Next is an effective method to prevent the shadow from influencing the calculations.

We can obtain the pseudo-center point of the pupil $(X_c, Y_c)$ by calculating the centroid of the dark pixel from the bi-level image threshold (see Fig. 5).

$$X_c = \sum \frac{x_i}{n}, \quad Y_c = \sum \frac{y_i}{n},$$

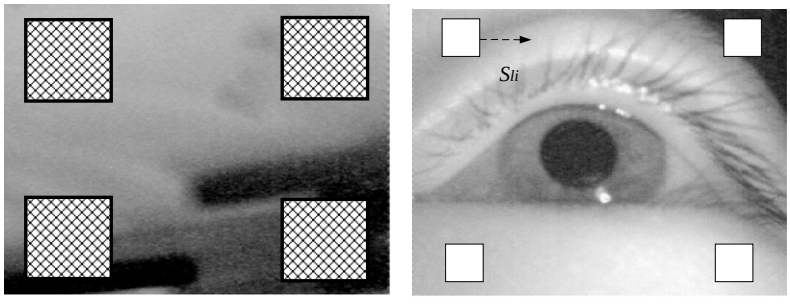


(a) (b)

Fig. 3. Four lattice images for operating condition detection: (A) No user is wearing the HMD in the pre-operation condition and (B) in use.

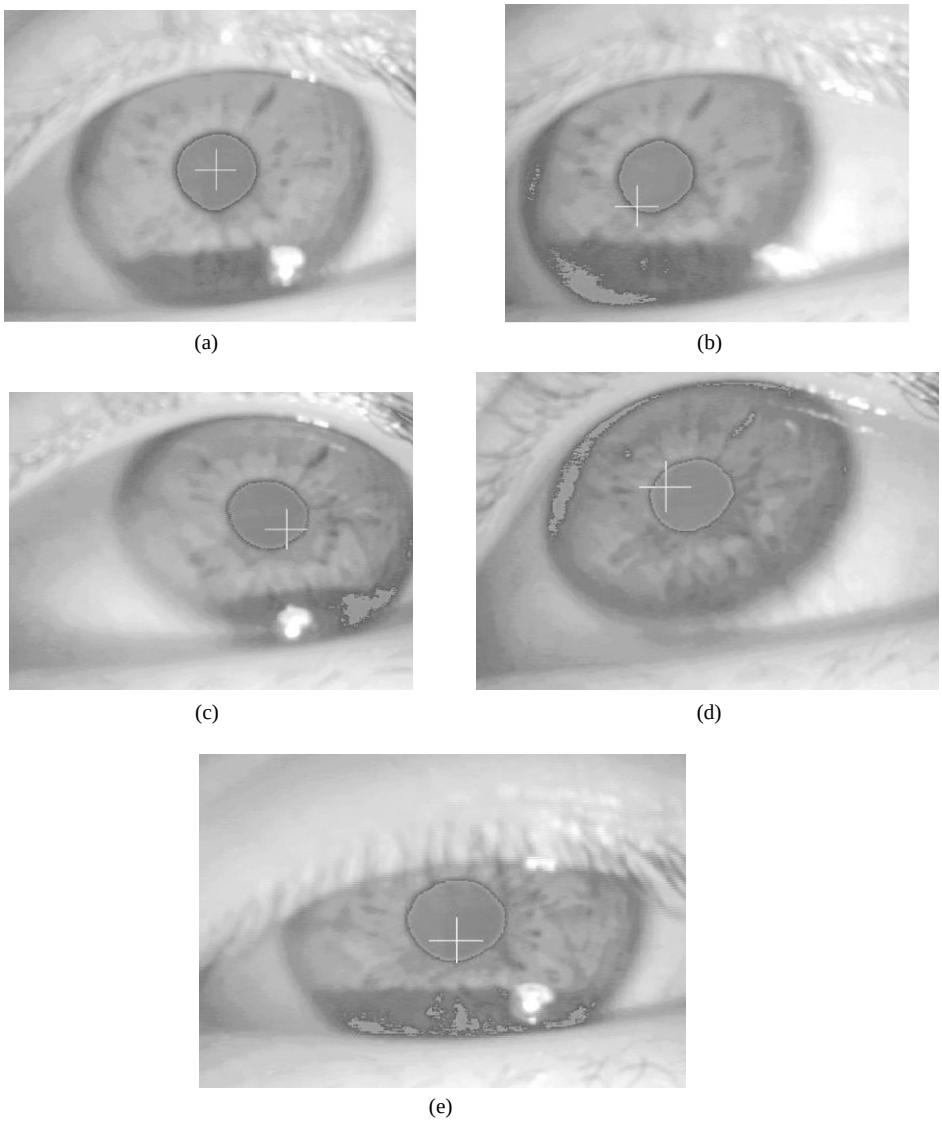

Fig. 4. The shadow appears when the user gazes at (A) the middle icon, (B) the left icon, (C) the right icon, (D) the top icon, and (E) the bottom icon.

where $x_i$ and $y_i$ are the $x$- and $y$-axis coordinates of a dark pixel, $n$ is the number of dark pixels. Assume that $D$ is the distance from the pseudo-center point of the pupil to a pixel $(x_i, y_i)$:

$$D = \sqrt{(X_c - x_i)^2 - (Y_c - y_i)^2}.$$

Let $R$ be the red color gray level of a pixel at the location $(x_i, y_i)$. Then set $R_s$ as the gray level value after the weighting operation and $r$ as an adjustable constant:

$$R_s = R + \frac{D}{r} \times \alpha, \quad \text{when } 5r > D > r,$$

$$R_s = R + r \times 5, \quad \text{when } D > 5r,$$

$$R_s = R, \quad \text{when } D < r.$$

A typical value for $r$ is in the range from 20 to 100 in our system. $\alpha$ is a weighting factor, $\alpha > 1$. Accordingly, the pixel in the pupil will obtain the value of $R_s$ smaller than a specified data.

### 2.3. Eye/HMD slide compensation

In practice, we found that the average brightness variation is not apparent if there is a slight slide between the eye and HMD. We can see that there is a distinct change in the lattice image histogram. The brightness distribution appears as a hierarchical distribution. As shown in Fig. 6, first we find the maximum number of pixels, $P_m$, in the lattice image histogram:

$$P_m = \max(P_i),$$

where $P_i$ is the number of pixels in the histogram.

Suppose that the corresponding gray level for $P_m$ in the histogram is $M$. We can threshold $M$ into two groups in the

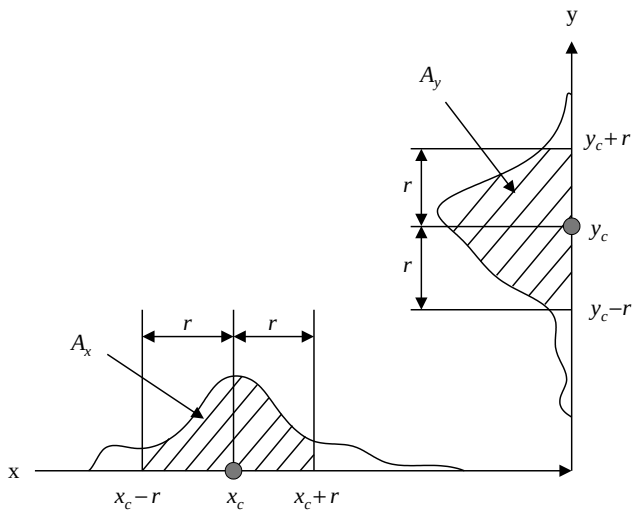


Fig. 5. The centroid $(x_c, y_c)$ of the projected area.

lattice image. Let $M_{lc}$ and $M_{rc}$ denote the first-order moment of the two groups:

$$M_{lc} = \frac{\sum_{i=1}^{M} iP_i}{N_1},$$

$$M_{rc} = \frac{\sum_{i=M}^{255} iP_i}{N_2},$$

where $i$ is the gray level, $N_1$ is the pixel number from gray level 0 to $M$ and $N_2$ is the pixel number from gray level $M$ to 255.

Let $P_{lc}$ and $P_{rc}$ denote the average number of pixels for the two groups:

$$P_{lc} = \frac{\sum_{i=1}^{M} P_i}{M},$$

$$P_{rc} = \frac{\sum_{i=M}^{255} P_i}{255 - M}.$$

Then, we obtain the angles $\theta_1$ and $\theta_2$ (as shown in Fig. 6):

$$\theta_1 = \cos^{-1} \frac{(M_{lc} - M_{rc})(M_{lc} - M) + (P_{lc} - P_{rc})(P_{lc} - P_m)}{\sqrt{(M_{lc} - M_{rc})^2 + (M_{lc} - M)^2}\sqrt{(P_{lc} - P_{rc})^2 + (P_{lc} - P_m)^2}},$$

$$\theta_2 = \cos^{-1} \frac{(M_{rc} - M_{lc})(M_{rc} - M) + (P_{rc} - P_{lc})(P_{rc} - P_m)}{\sqrt{(M_{rc} - M_{lc})^2 + (M_{rc} - M)^2}\sqrt{(P_{rc} - P_{lc})^2 + (P_{rc} - P_m)^2}}.$$

In our setup, the horizontal slide $S_{li}$ of the $i$th lattice image can be expressed as

$$S_{li} = K_1\Delta\theta_1 + K_2\Delta\theta_2 + K_3\Delta M.$$

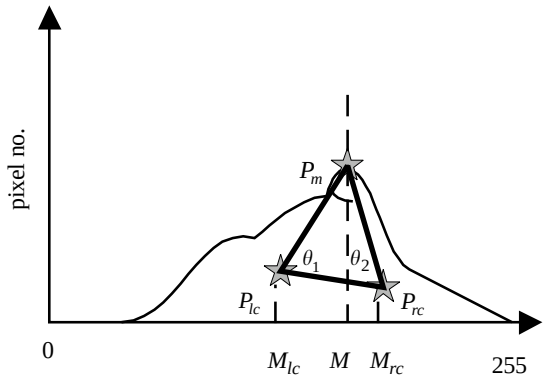


Fig. 6. The relation of $P_m$, $P_{lc}$ and $P_{rc}$.

The total horizontal slide $S_l$ can be obtained using the summation of the sub-slides of the four lattice images.

## 3. Experiments

### 3.1. The field depth

This measuring system provides an apparatus for measuring pupil dilation comprised of:

1. A removable and attachable image capturing device for capturing the image of the subjects' eyeball in real time.
2. An image capture card, for receiving and processing the eyeball images, calculating the position of the centroid of the pupil and the pupil area.
3. A computer for receiving and analyzing the data from the image capture card.
4. A PC to TV encoder box, which simultaneously displays a VGA signal both on the PC monitor and the HMD.
5. A switch used to select the VCR or the "VGA" image output to a compatible PC for the subject.

The light from the scene of the eye passes through the CCD camera and is collected by a condenser lens and directed toward the surface of a photodetector. The optical axis of the CCD camera is not perpendicular to the eye view (Fig. 7). It is important to evaluate the depth of the field in this system. A single equation can be used to determine the relationship between the eye and the image distances:

$$\frac{1}{S'} + \frac{1}{S} = \frac{1}{f}.$$

This means that the reciprocal of the eye distance, $S$, plus the reciprocal of the image distance, $S'$, equals the reciprocal of the focal length of the lens $f$.

Here we adopt $f = 5.5$ mm, so the following data are obtained:

When $S = 60$ mm, $S' = 6.05$ mm.
When $S = 70$ mm, $S' = 5.96$ mm.
When $S = 50$ mm, $S' = 6.17$ mm.

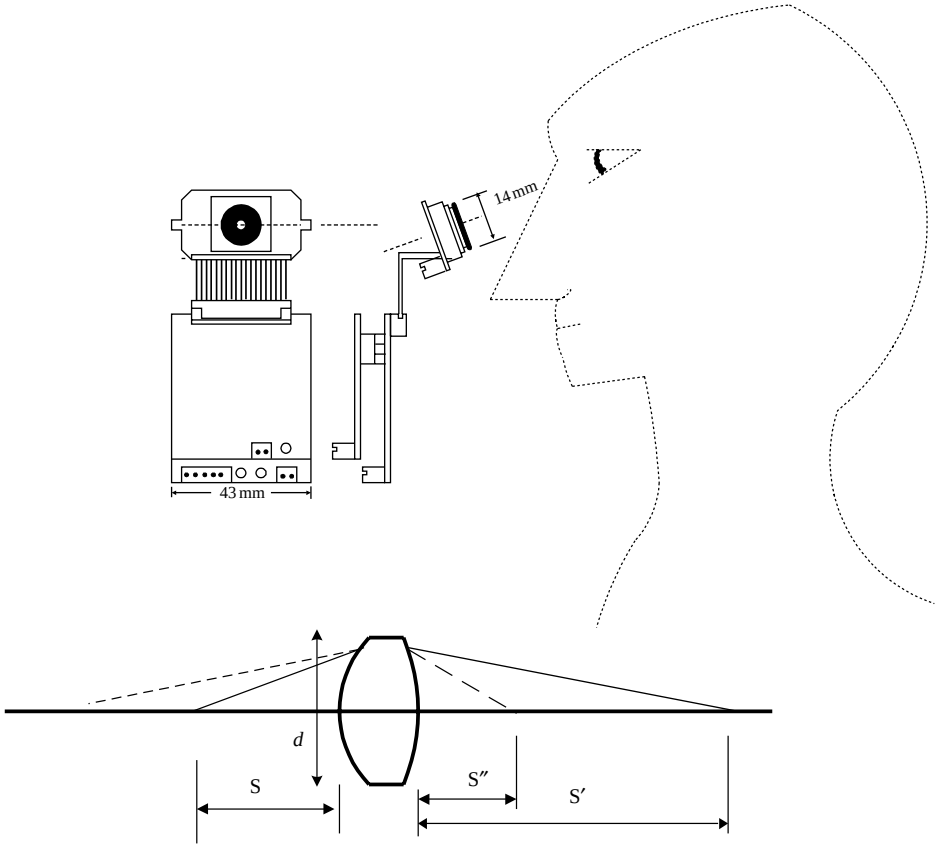


Fig. 7. The geometric relation of the CCD camera and the subject.

Suppose that the image plane is closer to the lens, at a distance $S''$, then the amount of blur $b'$ is given by [17]

$$b' = \frac{d(S' - S'')}{S'},$$

where $d$ is the diameter of the lens aperture.

Let the maximum acceptable blur diameter be $b$. Then the depth of field, $D$, is the difference between the near and far plane distances:

$$D = \frac{2bdfz(f+z)}{d^2f^2 - b^2z^2},$$

where $z = \mathrm{d}f/b$, called the hyperfocal distance. The depth of the field in our system is about 25 mm.

In this measuring system, the VCR and display provide video signals to an observer. At the same time, the pupil image video signals are transmitted to the computer to calculate the pupil area and transfer the diameter of the pupil [18,19]. Here we tested this pupillary response measuring system using the following simple experiments. The system is set up in a dark room, but the tester was first sent out for 15 min to ensure that the experiment might begin with light-adapted eyes. From the beginning to the end of the experiment, the visual fatigue and concentration detection lasted at 2–3 min intervals.

### 3.2. Visual fatigue detection

Visual fatigue estimations have been obtained by autoregressive modeling over 100 consecutive samples. A fatigued eye exhibits a reduction in visual mechanism responsiveness as a direct result of stimulation. This is a phenomenon that has been investigated experimentally using the relationship in the variation in the pupil diameter or pupil's area $a_v$. Let

$$a_v = a_n - \frac{\sum_{i=1}^{n-1} a_i}{n-1}.$$

where $a_v$ is the variation in the pupil area, $a_n$ is the average pupil area during the $n$th period, $a_i$ is the average pupil area during the $i$th period, and $n$ is the number of periods.

If the value of $a_v$ is larger than a threshold value, we infer that the subject is fatigued.

When the period is short, the variation in the pupil area provides useful information for distinguishing blinking from other motions of the eye.

Let $n_{\mathrm{bl}}$ denote the amount of eye blink and we obtain

$$n_{\mathrm{bl}} = n'_{\mathrm{bl}} + 1 \quad \text{when } a_n \cong 0 \text{ and } a_v > 0,\ a'_v < 0,$$

where $n'_{\mathrm{bl}}$ and $a'_v$ are the number of eye blinks and the variation in the pupil area in the last time.

### 3.3. Concentration detection

In a concurrent pupil measuring system study validation, the pupillary response and location information were obtained simultaneously. The location information with concurrent test validity evidence is usually desirable for achievement tests in our system. Let

$$a_1 = \frac{\sum_{i=1}^{N} x_i}{N}, \quad a_2 = \frac{\sum_{i=1}^{N} y_i}{N},$$

$$X = \frac{\sum_{i=1}^{n_1} x_i}{n_1}, \quad \text{when } (x_i - a_1) \leqslant 10,$$

$$Y = \frac{\sum_{i=1}^{n_2} y_i}{n_2}, \quad \text{when } (y_i - a_2) \leqslant 10,$$

where $a_1$ is the average value of $x$-axis coordinate, $a_2$ is the average value of $y$-axis coordinate, $N$ is the number of image sequences, $X$ is the $x$-axis coordinate of the gaze point, $Y$ is the $y$-axis coordinate of the gaze point, $n_1$ is the number $(x - a_1) \leqslant 10$ in the image sequence, and $n_2$ is the number $(y - a_2) \leqslant 10$ in the image sequence.

We can calculate the centroid $(x_c, y_c)$ of the projected area (Fig. 5).

$$x_c = \frac{\sum_{i=1}^{n} x_i}{n}, \quad y_c = \frac{\sum_{i=1}^{n} y_i}{n},$$

$$A_x = \frac{n_x}{n}, \quad A_y = \frac{n_y}{n},$$

where $n$ is the total number of the image sequence. $n_x$ is the case number $x_c - r < x_i < x_c + r$, $n_y$ is the case number $y_c - r < y_i < y_c + r$, $A_x$ is the $x_c - r < x_i < x_c + r$ ratio to the total area, $A_y$ is the ratio of the $y_c - r < y_i < y_c + r$ area to the total area.

The ratio $A_x$ and $A_y$ can be used to detect the subject's concentration level. The values $A_x$ and $A_y$ must be larger than the threshold value to ensure that the experimental result is valid.

## 4. Results and discussion

### 4.1. Results of simultaneous contrast experiment

The interesting phenomena that the vision system exhibit related to brightness are the Mach Band effect and the simultaneous contrast. This phenomenon clearly demonstrates that perceived brightness to the eye is not a simple function of intensity. In the test patterns (Fig. 8(a)–(d)) for the simultaneous contrast viewing pattern experiments, different contrasts but of the same brightness in the center square were presented. This means that the center squares had exactly the same intensity, but they appeared progressively lighter as the background became darker. The screen was replaced by a totally bright picture for an interim and then refreshed the eye the next pattern for 5 s period. The illumination of the square was held constant and the intensity of the background diminished with the contrast allowed to vary incrementally. The results of the experiment are shown in Fig. 9. We can see that the pupillary response actually varies based on the average brightness observed.

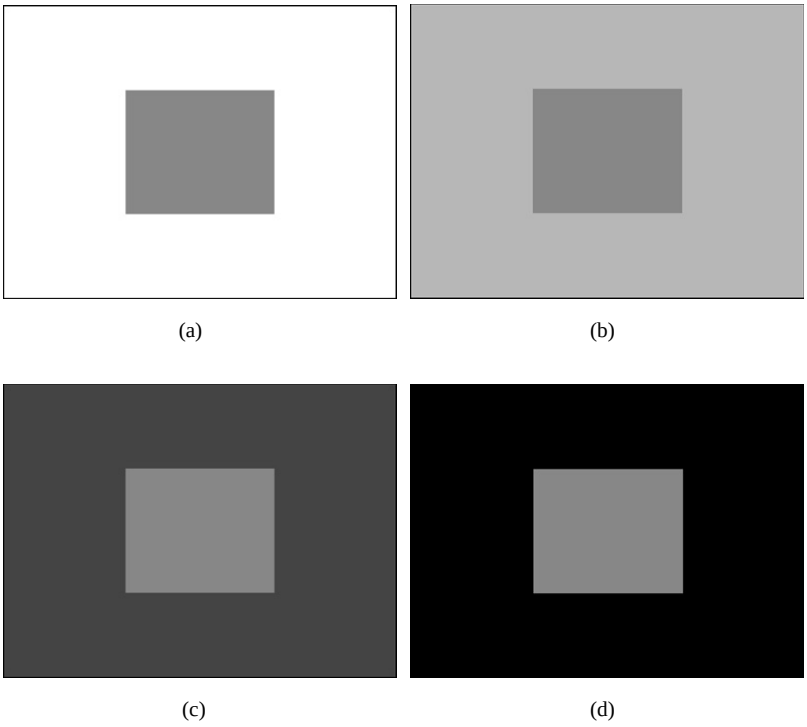


Fig. 8. The test pattern for different contrast viewing pattern experiments.

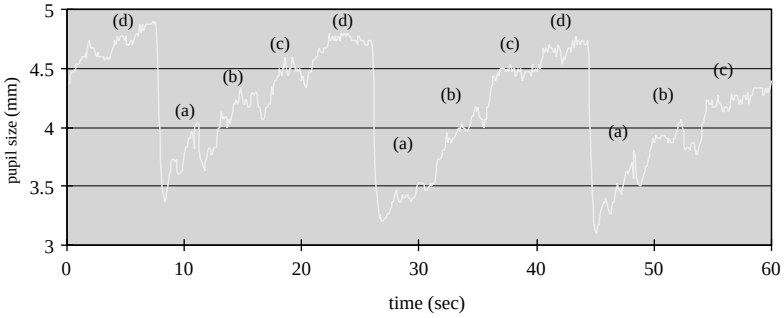


Fig. 9. Different contrast viewing pattern experimental results.

| No. | (1) | (2) | (3) | (4) | (5) | (6) | (7) | (8) | (9) | (10) |
|---|---|---|---|---|---|---|---|---|---|---|
| image | | | | | | | | | | |
| brightness | 0 | 28 | 56 | 85 | 112 | 142 | 170 | 198 | 227 | 255 |

Fig. 10. The test pattern for the different brightness viewing pattern experiments.

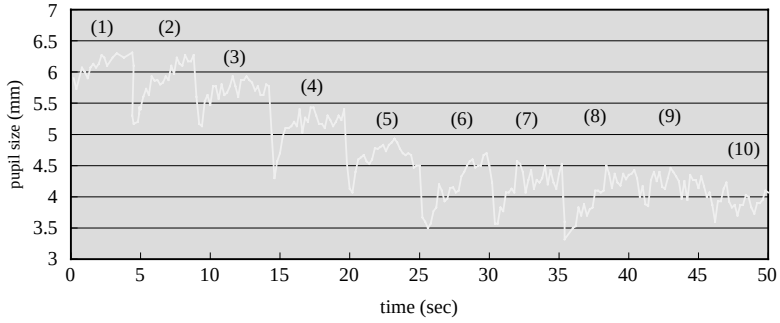


Fig. 11. Different brightness viewing pattern experimental results.

### 4.2. Different brightness viewing patterns

The human vision system responds to a wide range of brightness levels. It is well known that the pupil diameter is a function of the ambient illumination. Instead of keeping the eye in the dark or in bright long enough to obtain practically complete dilation, we exposed the eye to different brightness levels at short intervals (5 s). Fig. 10 represents the test pattern for the different brightness viewing pattern experiments. The experimental results are shown in Fig. 11. The pupil diameter varied from 3.5 to 6.5 mm, and was limited by the dark threshold and glare limit.

### 4.3. Different contrasts with same average brightness viewing patterns

Fig. 12 represents the test patterns for the different contrast and same average brightness viewing pattern experiments. As shown in Table 1, let the background brightness be $I_1$, the brightness of the square $I_2$. Then the image contrast depends on $\Delta I$.

$$\Delta I = I_2 - I_1.$$

If the object area is $A_2$ and the background area is $A_1$, we can obtain the average brightness $\bar{I}$ of the whole image

$$\bar{I} = \frac{I_1 \cdot A_1 + I_2 \cdot A_2}{A_1 + A_2}.$$

The average brightness of all of the testing patterns is 127, as shown in Fig. 12. Fig. 13 shows the different contrast and same average brightness viewing pattern experimental results (see Table 1).

### 4.4. Selective adapts to spatial frequencies and contrast

To determine a subject's selective adaptation to spatial frequencies and contrast, the subject looks at a grating of the same brightness for about 5 s. Then the screen is refreshed and the subject looks briefly at the next test grating. Fig. 14 represents the test patterns for the straight grating

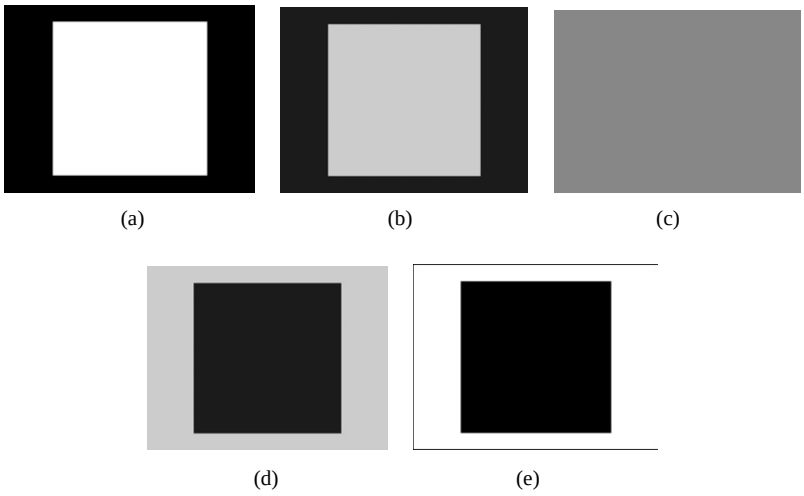


Fig. 12. The test patterns for different contrast and same average brightness viewing pattern experiments.

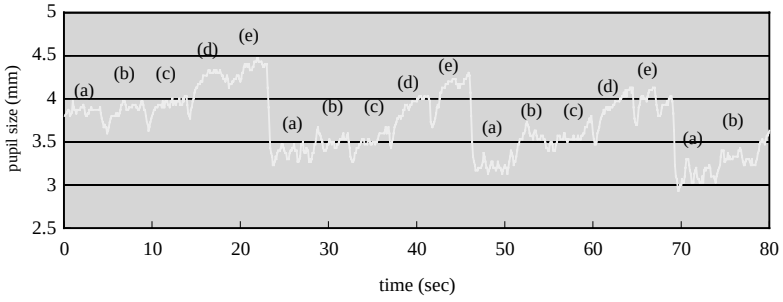


Fig. 13. The different contrast and same average brightness viewing pattern experimental results.

Table 1
The brightness of the background and the object

| Image no. | Brightness of background ($I_1$) | Brightness of object ($I_2$) | $\Delta I$ |
|---|---|---|---|
| (a) | 0 | 255 | 255 |
| (b) | 63 | 191 | 128 |
| (c) | 127 | 127 | 0 |
| (d) | 191 | 63 | −128 |
| (e) | 255 | 0 | −255 |

Table 2
The brightness of the fringes in grating

| Image no. | Brightness of dark fringe ($I_1$) | Brightness of white fringe ($I_2$) | $\Delta I$ |
|---|---|---|---|
| (a) | 127 | 127 | 0 |
| (b) | 95 | 159 | 64 |
| (c) | 63 | 191 | 128 |
| (d) | 31 | 223 | 192 |
| (e) | 0 | 255 | 255 |

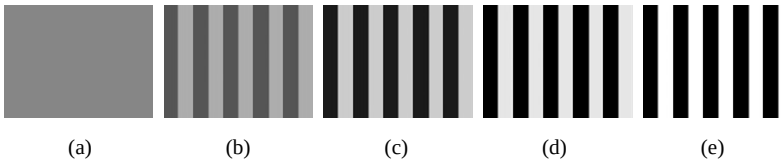


Fig. 14. The test patterns for straight grating view experiments.

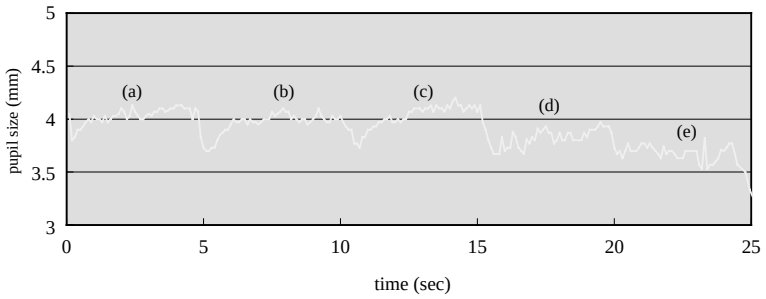


Fig. 15. The straight grating view experiment results.

Table 3
The fatigue detection and concentration evaluation

| Time | The number of eye blink, $n_{bl}$ | The variation in the pupil area, $a_v$ (mm$^2$) | Ratio $A_x$ | Ratio $A_y$ |
|---|---|---|---|---|
| 1 min | 9 times/min | 0 | 100 | 100 |
| 30 min | 12 times/min | 0.723 | 98.5 | 96.2 |
| 60 min | 14 times/min | 0.211 | 95.1 | 94.4 |
| 120 min | 14 times/min | −0.117 | 86.2 | 85.9 |
| 180 min | 20 times/min | −0.025 | 84.2 | 83.8 |
| 240 h | 23 times/min | 0.512 | 75.2 | 74.3 |

experiments. As shown in Table 2, the brightness is $I_1$ in the dark fringe and $I_2$ in the white fringe. The average brightness of the whole image was 127. Fig. 15 shows the results from viewing the straight grating experiments. We can see that there is about 0.5 mm variation in the diameter of the pupil.

### 4.5. Fatigue detection and concentration evaluation

Fatigue detection and concentration evaluation can be done by analyzing the differences in pupil area and locations in successive eye images. Table 3 shows an example of a user engaged in a long-time reading task. The variation in the pupil area $a_v$ reveals the task is heavy or easy. When the text is complicated or the pattern is in low contrast, the value of $a_v$ will be positive. When the user feels fatigued, the number of eye blinks increase and the ratios $A_x$, $A_y$ decrease.

## 5. Conclusion

A new image-processing method to calculate the location and size of the pupil in an image with an inexpensive optical hardware was proposed. This system comprised of heads-up display (HMD) and eye-tracking device, allows detection under different conditions. This system evaluates the operating conditions of the subject, whether the adjustment is correct, and guides the operator in using the system. The experiments used to verify the pupillary response used a new image-processing method. Additional experiments and system verification are needed. This measurement system will provide more understanding about pupil behavior and response. The data can also provide quantified information for ophthalmology and psychology use.

## Acknowledgements

This work was sponsored by the National Science Council, Chung-Shan Institute of Science & Technology, Taiwan, Republic of China, under grant number NSC90-2614-H-035-001-F20 and BV91U14P.

## References

[1] Myers GA, Sherman KR, Stark L. Eye monitor—microcomputer-based instrument uses an internal model to track the eye. IEEE Comput 1991;24(3):14–21.
[2] Kirby M, Sirovich L. Applications of the Karhunen–Loeve procedure for the characterization of human faces. IEEE Trans Pattern Anal Mach Intell 1990;12(1):103–8.
[3] Yankang Wsng, Hideo Kuroda, Makoto Fujimura Nakamura. Automatic extraction of eye and mouth fields from monochrome face image using fuzzy technique. Fourth IEEE International Conference on Universal Personal Communications (ICUPC'95), Tokyo, Japan, 1995. p. 778–82.
[4] Chern-Sheng Lin, Chih-Chung Chien, Nanjou Lin, Chiao-Hsiang Chen. The method of diagonal-box checker search for measuring one's blink in eyeball tracking device. Opt Lasers Technol 1998;30(5):295–301.
[5] Wagner R, Galiana HL. Evaluation of three template matching algorithms for registering images of the eye. IEEE Trans Biol Eng 1992;39(12):1313–9.
[6] Spindler F, Chaumette F. Gaze control using human eye movement. IEEE International Conference on Robotics and Automation, Albuquerque, NM, USA 1997. pp. 2258–63.
[7] Grattan KT, Palmer AW. Interrupted reflection fiber optic communication device for the severely disabled. J Biomed Eng 1984;6:321–2.
[8] Grattan KT, Palmer AW, Sorrell. Communication by eye closure—a microcomputer-based system for the disabled. IEEE Trans Biomed Eng 1986; BME33:977–82.
[9] Robert J. Gregory. Psychological testing: history, principles, and applications, 2nd ed. Boston: Allyn and Bacon Publishing Corp, 1996. p. 4641.
[10] Stewart DW. Physiological measurement of advertising effects. Psychol Marketing 1984;1:43–8.
[11] John M. Darley, Sam Glucksberg, Ronald A. Kinchla. Psychology, 5th ed. Englewood Cliffs, NJ: Prentice-Hall Press, 1991. p. 85–93.
[12] Xie X, Sudhakar R, Zhuang H. A cascaded scheme for eye tracking and head movement compensation. IEEE Trans Syst Man Cybern 1998;28(4):487–90.

[13] Martin CF, Schovance L. A control model of eye movement. Conference on Decision & Control, San Diego, CA, USA, 1997. p. 1135–9.
[14] Allison RA, Eizenman M, Cheung BSK. Combined head and eye tracking system for dynamic testing of the vestibular system. IEEE Trans Biol Eng 1996;43(11):1073–82.
[15] Talmi K, Liu J. Eye and gaze tracking for visually controlled interactive stereoscopic displays. Signal Process: Image Commun 1999;14:799–810.
[16] Pastoor S, Liu J, Renault S. An experimental multimedia system allowing 3-D visualization and eye-controlled interaction without user-worn devices. IEEE Trans Multimedia 1999;1(1):41–52.
[17] Jain R, Kasturi R, Schunck BG. Machine vision. New York: McGraw-Hill Corp, 1995. p. 252–3 [chapter 8].
[18] Chern Sheng Lin. An eye behavior measuring device for V.R. System. Opt Lasers Eng 2002;38(6):13–39.
[19] Chern Sheng Lin, Kai-Chieh Chang, Young-Jou Jain. Opt Lasers Technol 2002;34(5):405–13.